15.6 LOCAL SCALING OF TURBULENCE IN THE STABLE INTERNAL BOUNDARY LAYER AROUND A COASTAL HEADLAND

Stefan Söderberg*
Stockholm University, Stockholm, Sweden

Ian M. Brooks
Scripps Institution of Oceanography, La Jolla, California

Michael Tjernström
Stockholm University, Stockholm, Sweden

1. INTRODUCTION

The coastal zone, a region that may extend up to 100 km both inland and offshore of the coastline, is characterized by a step-change in surface conditions, e.g., roughness, temperature, moisture, and orography. The contrast in surface conditions results in a complex environment with significant spatial and temporal variability.

During summertime, the prevailing winds off northern California and Oregon are northwesterly. Subsidence maintains a strong inversion that slopes towards the coast and the boundary layer (BL) flow is confined by the coastal mountains. Dorman et al. (2000) found the flow to be close to supercritical over an extensive region and supercritical as it rounds each cape and headland where it diverges and accelerates to form an expansion fan. In this highly heterogeneous environment, the marine air-mass is brought over cool, upwelling coastal waters resulting in the formation of stable internal boundary layers (IBL).

For the stable boundary layer there is, as yet, no universally applicable theoretical framework. Local similarity scaling (Nieuwstadt 1994; Sorbjan 1986, 1987) is a promising approach. It has been applied successfully in a number of studies of coastal BL's. General applicability has, however, not yet been demonstrated.

This study investigates the turbulence structure and local scaling within a stable BL around a coastal headland off northern California using aircraft observations and numerical simulation.

2. MEASUREMENTS

As part of the Coastal Waves '96 field program (Rogers et al. 1998), the NCAR C-130 Hercules performed 11 research flights during the month of June off the coast of California. In this study we use data from a flight around Cape Mendocino on June 7. The flight track for this day is shown in Figure 1.

The primary objective of the campaign – to map the mesoscale structure of the BL – only allowed time for 30-m turbulence flight legs for most flights. However, the large number of sawtooth profiles carried out from ~15m to above the inversion provide an alternative source of turbulence information (Mahrt 1985; Lenschow et al. 1988; Tjernström 1993).

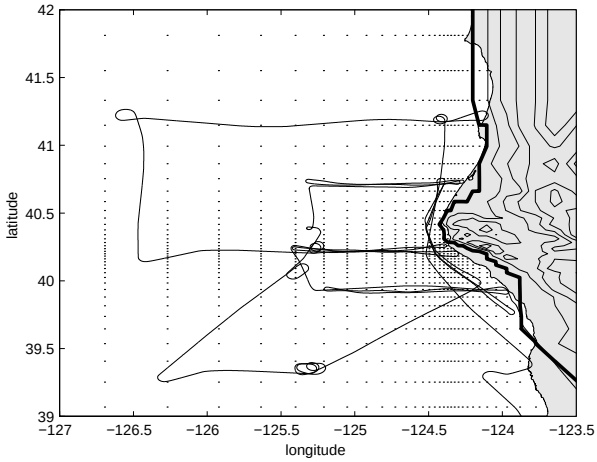

Figure 1. Aircraft flight track is shown by the solid line. Model grid is indicated by dots, model terrain is contoured at 200m.

3. MODEL DESCRIPTION AND SETUP

The model we utilize is the Uppsala University mesoscale model, a 3D hydrostatic, non-linear, primitive equations model. The turbulence closure is a modified level-2.5 closure (Mellor and Yamada 1982), including a correction for non-realizable 2nd-order moments, and an improved formulation for the pressure redistribution terms in the TKE equation – the "wall correction" (Andrén 1990). A more detailed discussion of the model and what we can really expect to learn from looking at modeled turbulence is found in the companion poster-presentation, P6.4.

Initial conditions were set up to match observations upstream of Cape Mendocino; the MBL was assumed well-mixed and capped by a strong inversion, the low-level background flow was set northerly. Observed SST was used and held constant in time. The vertical grid expands log-linearly with height, from a resolution of ~6 m at the surface to ~150 m at the model top. Model terrain and the horizontally expanding grid are shown in Figure 1. The model results presented here were initialized 1800 LT on the day preceding the event, around 1500 LT.

**Corresponding author address:* Stefan Söderberg, Dept. of Meteorology, Stockholm University, SE-106 91 Stockholm, Sweden; email: stefan@misu.su.se

4. RESULTS

Before examining the turbulence structure the mean structure of the BL will be considered. Observed BL depth and 30-m wind field are shown in Figure 2. In the lee of Cape Mendocino, where the observed SST is the lowest, the BL collapses. The axis of the accelerating jet around the cape is coincident with the region of maximum gradient in BL depth. The model reproduces the structure of the collapsing BL and the observed wind field well in most respects (not shown).

Figure 3 shows examples of observed and modeled profiles of potential temperature and wind speed at the two locations marked in Figure 2a. All model profiles covering the horizontal range of the slanting aircraft profiles are plotted for a better comparison. Within the limits of the model's vertical resolution (~100 m at BL top) the BL depth at point A, is accurately captured. But, the observations indicate a ~300 m deep IBL and a nearly constant wind speed from the top of the IBL to the inversion base which the model does not capture. At point B, within the expansion fan, the BL depth is captured but the inversion is deeper and has a slightly weaker gradient. The discrepancies between the model and observation may be due, at least in part, to the finite vertical resolution of the model, but also suggest that the mixing within the model is too efficient.

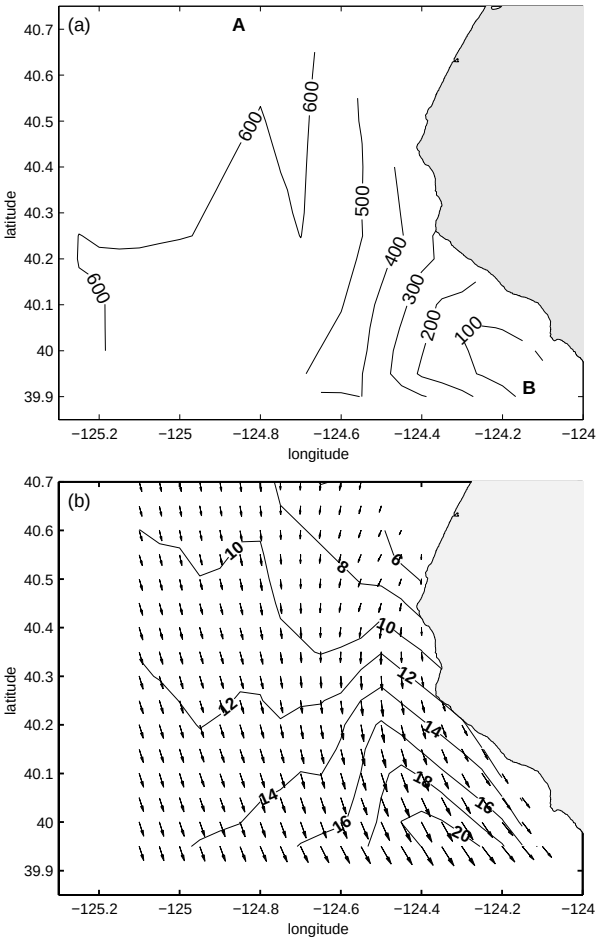

Figure 2. Observed (a) BL depth, and (b) near-surface wind field. The points A and B on (a) mark the locations of the profiles shown in Fig. 3.

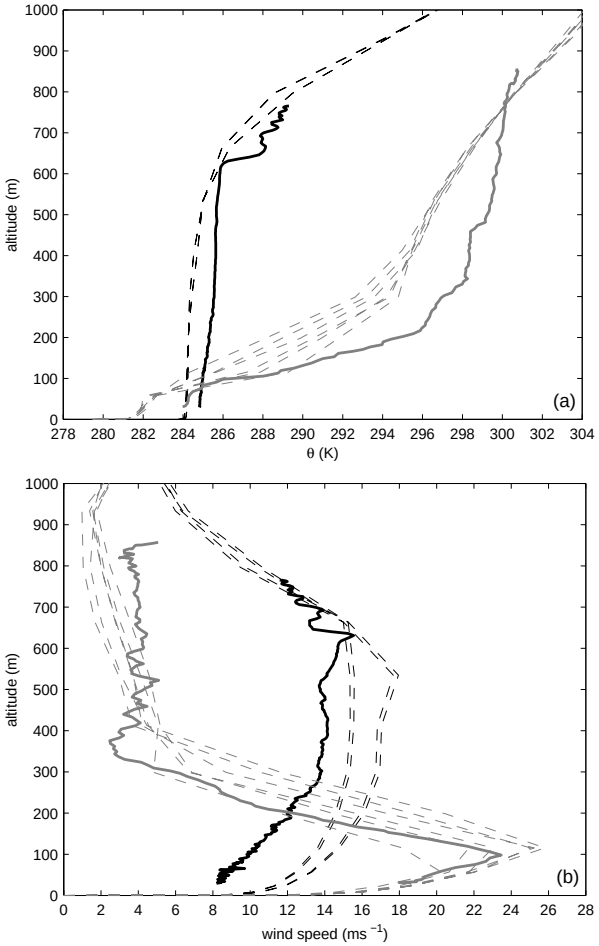

Figure 3. (a) Profiles of potential temperature at A (dark line) and B (gray line). Dashed lines are model profiles. (b) As (a) but for wind speed.

Upstream of the cape, observed turbulence is largely confined to the IBL while the model produces turbulent mixing throughout the BL. In the region of the expansion fan, significant turbulence was observed above the collapsed BL; this corresponds to a region of upward momentum flux found in the numerical simulation above the near-coast side of the jet (not shown).

From here, the focus will be on local scaling. The similarity scales are defined in a similar way as in the Monin-Obukhov scales, but depend upon local turbulence quantities at the measurement height instead of surface values:

$$u_L(z) = [\,\overline{w'u'}^2 + \overline{w'v'}^2\,]^{1/4} \quad (1a)$$

$$L_L(z) = -u_L^3 / \left[\kappa\beta\overline{w'\theta_v'}\right] \quad (1b)$$

Figure 4 shows the scaled standard deviation of vertical velocity profiles plotted against the stability parameter z/L_L. Data from the continuously turbulent IBL is included from all available profiles divided into those

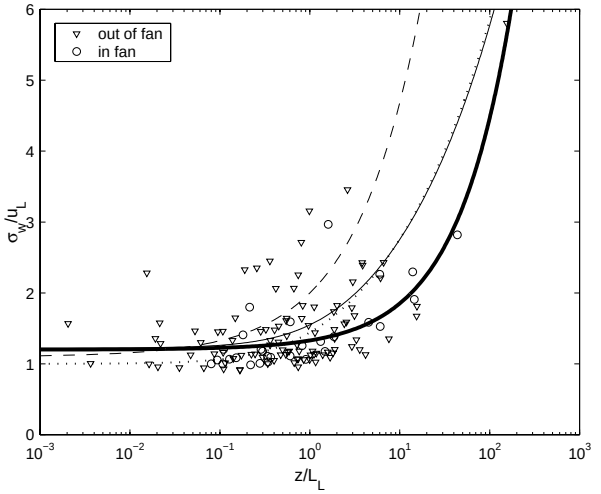

Figure 4. Standard deviations of the vertical velocity scaled by the u_L plotted against the stability parameter z/L_L. Solid thick line is a best fit to our entire dataset, other lines are fits to Pahlow et al. (2001)(dashed), Shao and Hacker (1990)(dotted), Al-Jiboori et al. (2002)(thin solid).

obtained within the expansion fan (triangles) and those from the undisturbed flow outside the fan (circles). There is a significant scatter in the data but there is no systematic difference between them. The thick solid line is the best fit to our dataset. Also shown are the fits obtained by Shao and Hacker (1990), Pahlow et al. (2001), and Al-Jiboori et al. (2002). The four data sets show similar behavior although substantial differences are found between some of the curves at high stabilities; this is, however, within the scatter of the present data. For stabilities in the range $0.1< z/L_L <5$ all curves lie close to, and pass through, the value of 1.4 suggested by Nieuwstadt (1994) as a constant for σ_w/u_L.

The modeled BL vertical velocity variances, scaled in the same way as in Figure 4, are shown in Figure 5; dashed line is the best-fit curve from the observations. It is clear that the same scaling applies to both observed

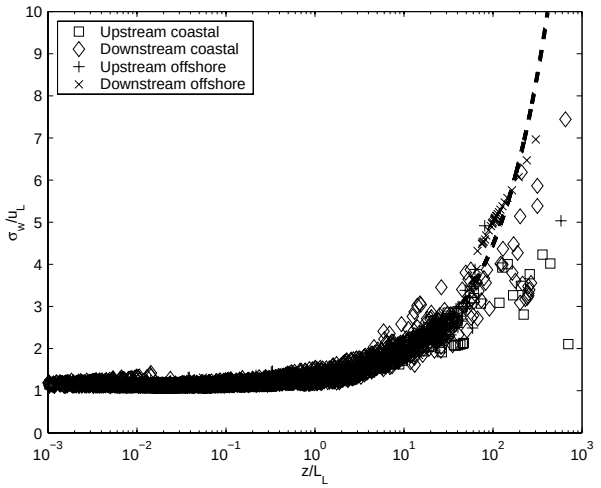

Figure 5. Scaled standard deviations of the vertical velocity from the model. Dashed line is the best fit curve from the observations.

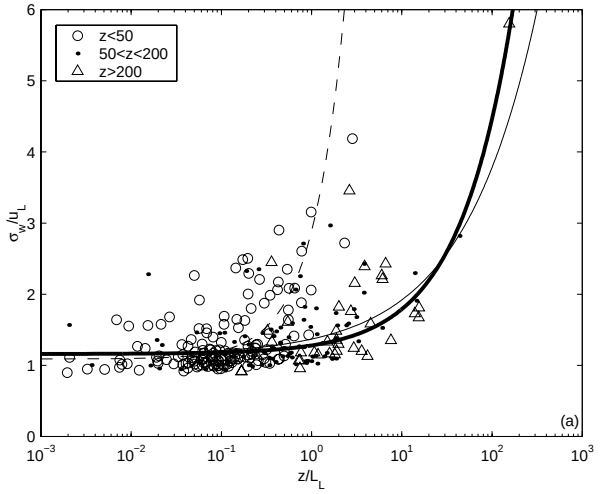

Figure 6. Scaled standard deviations of vertical velocity partitioned by altitude. Best-fit curves: z<50 - dashed; 50≤z≤200 - thin solid; z≥200 - heavy solid.

and modeled turbulence. Of note is the fact that the scaling shows no discernable changes across the whole region, in the spite of the substantial changes in mean flow conditions and turbulence intensity. A more in depth discussion on the ability of the model to simulate the turbulence statistics correctly is found the companion poster-presentation, P6.4. Here we conclude that the close agreement between the modeled and observed local scaling functions provides a verification of the validity of the turbulence closure used in the model.

The difference between the scaling function obtained here and the one found by e.g. Pahlow et al. (1990) poses the question if there is a real difference in the scaling between the flows. If this is the case, the local scaling cannot be considered universal in its present form. A significant difference between the studies is that our data span the entire BL while Pahlow et al.'s were obtained within 5 m of the surface. The effect of altitude is illustrated in Figure 6, here the scaled vertical velocities have been divided into three groups, z<50, 50≤z<200, and z≥200 m. For near-neutral conditions, all three curves approach a value close to 1.1. However, the curve for the low-level data rises much faster than that for high or mid-level data, which both are very similar to the entire data set curve fit. Similar results are obtained for the along-stream velocity (not shown). Thus, the observed differences in scaling behavior may be related to the proximity to the surface. However, one possibility is that the change in scaling behavior is an artifact of the distribution of stability with altitude. Since the strongest mixing will take place near the surface, where shear generation of turbulence is strongest, the near-surface data will only be weakly stable. From the observations we find that the maximum stability for the z<50 m group is, z/L_L~3, the highest stabilities are only found in the upper part of the turbulent layer. The lack of high-stability data near the surface may therefore bias

the low-level function. Model data from different height intervals occupy different portions of the z/L_L axis but all fall close to the empirical best-fit line. But, differences between our results and those of the other studies included in Figure 4 cannot be explained by simple sampling bias between the subsets of data. This once again poses the question if local similarity theory is adequate in its present form.

5. DISCUSSION

The turbulence structure in a stable BL around a coastal headland have been investigated using aircraft observations and numerical modeling. The model was able to reproduce the observed mean state of the BL in most respects. Observed turbulence was generally confined to a stable IBL whereas the model produced a continuously turbulent BL.

Observed and modeled BL velocity variances, scaled with local similarity scales, agreed surprisingly well. This lends credibility to the turbulence closure used in the model. Noteworthy is that several observational studies have found similarly shaped functions for the scaled velocity variances, however, none have explained why these functions differ from the constant value predicted by Nieuwstadt's original theory. At least one of the assumptions this theory is based on - the assumption of spatial homogeneity - is certainly invalid in the present study, and for that of Shao and Hacker.

We hypothesize that the form of the observed similarity functions is due to a controlled breakdown of true local scaling under the influence of non-negligible non-local transport terms such as advection and turbulent transport terms in the TKE budget. These non-local processes may differ significantly between different sets of observations, while behaving in a well-defined manner for a particular environment. Thus, empirical functions may differ significantly between studies since the precise form depends on non-local properties of the flow. Figure 7 shows local scaling applied to all turbulent model points and observations above the BL top. Interesting to see is that although the well defined functional relationship appears to have broken down, the scaled variances are limited on the high side by the best-fit curve from the observations and on the lower side by a constant value near the neutral limit of the scaled variance. Following our hypothesis, this distribution can be interpreted as being due to a wide degree of variation in non-local transport properties among the points. The highest concentration of points lies close to the constant defined by neutral conditions representing conditions where turbulent processes are truly local; other sets of points that appear to lie along curves of similar shape should then represent locations with very similar non-local transport.

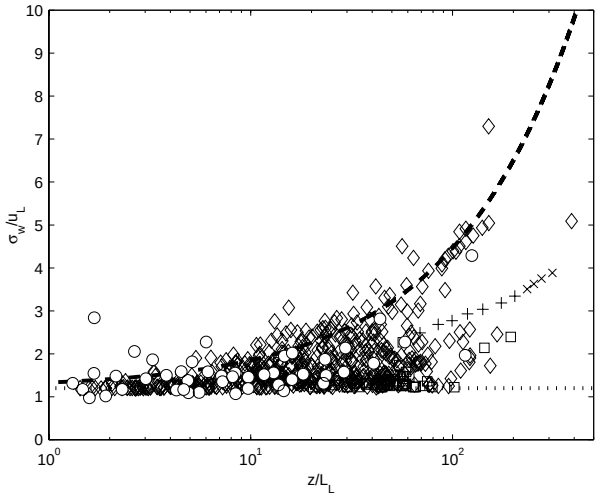

Figure 7. As Figure 5 but for points above the modeled BL top. Dashed line is best-fit curve from observations, dotted line is the constant value approached at near-neutral conditions. Included are also observations from above the BL top (circles).

Our results suggest that a reassessment of local similarity scaling should be carried out in order to examine the relationship between the scaling functions and non-local properties of BL flows. A more detailed analysis with a more extensive data set is needed.

REFERENCES

Al-Jiboori, M. H., Y. Xu, and Y. Qian, 2002: Local similarity relationships in the urban boundary layer. *Bound.-Layer Meteor.*, **102**, 63-82.

Andrén, A., 1990: Evaluation of a turbulence closure scheme suitable for air-pollution applications. *J. Appl. Meteor,* **29**, 224-239.

Dorman, C. E., T. Holt, D. P. Rogers and K. Edwards, 2000: Large-Scale Structure of the June-July 1996 Marine Boundary Layer Along California and Oregon. *Mon. Wea. Rev.*, 128, 1632-1652.

Lenschow, D. H., C. J. Zhu, and B. B. Stankov., 1988: The stably stratified boundary layer over the great plains I: Mean and turbulence structure. *Bound.-Layer Meteor.*, **42**, 95-121.

Mahrt, L., 1985; Vertical structure in the very stable boundary layer. *J. Atmos. Sci.*, **42**, 2333-2349.

Mellor, G. L., and T. Yamada, 1982: Development of a closure model of geophysical flows. *Reviews of Geophysics and Space Physics*, **20**, 851-875.

Nieuwstadt, F. T. M., The turbulent structure of the stable, nocturnal boundary layer. *J. Atmos. Sci*. **41**, 2202-2216, 1984.

Pahlow, M., M. B. Palange, and F. Porté-Agel, 2001: On Monin-Obukhov similarity in the stable atmospheric boundary layer. *Bound.-Layer Meteor.*, **99**, 225-248.

Rogers, D. P., and Coauthours, 1998: Highlights of Coastal Waves 1996. *Bull. Amer. Meteor. Soc*.,**79**, 1307-1326.

Shao, Y., and Hacker, J. M., 1990: Local similarity relationships in a horizontally inhomogeneous boundary layer, *Bound.-Layer. Meteor.*, **52**, 17-40.

Sorbjan, Z., 1986: On similarity in the atmospheric boundary layer, *Bound.-Layer Meteor*., **34**, 377-397.

Sorbjan, Z., 1987: An examination of the local similarity theory in the stably stratified boundary layer, *Bound.-Layer Meteor.*, **38**, 63-71.

Tjernström, M., 1993: Turbulence length scales in stably stratified free shear flow analyzed from slant aircraft profiles, *J. Appl. Met.*, **32**, 948-963.